Research Article

Xiaohong Jiang*, Zhongfei Shen, Bin Shen, Ying Sun

Preparation and pharmacodynamic evaluation of sodium aescinate solid lipid nanoparticles

https://doi.org/10.1515/chem-2023-0201
received August 10, 2023; accepted February 5, 2024

Abstract: Recent advancements in nanotechnology have spotlighted lipid nanocarriers as potent mediums for drug delivery, with solid lipid nanocarriers (SLNs) emerging as a key focus due to their unique structural attributes. This research specifically addresses the development and evaluation of the anti-inflammatory properties of SLNs loaded with sodium aescinate. To identify the most effective composition, a detailed pseudo-ternary phase diagram was employed. The production process of these SLNs involved sophisticated high-pressure homogenization techniques. For characterization, the average particle size and zeta potential were precisely measured using advanced laser diffractometry. Additionally, to ascertain the effectiveness of the drug encapsulation, the SLNs underwent a rigorous high-speed centrifugation process, enabling accurate determination of both the encapsulation efficiency and drug-loading capacity. The results of this research reveal that a relatively refined method for determining sodium aescinate content has been established, and a reasonable formulation has been selected for the preparation of sodium aescinate solid lipid nanoparticles. The average particle size was 142.32 ± 0.17 nm, the zeta potential was 1.60 ± 0.32 mV, and the encapsulation rate was 73.93 ± 4.65%. The drug loading was 13.41 ± 1.25%. In conclusion, this method can produce stable solid lipid nanoparticles containing sodium aescinate with uniform particle size, even distribution after encapsulation, and significant anti-inflammatory activity.

Keywords: sodium aescinate, solid lipid nanoparticles, high pressure homogenization method

*** Corresponding author: Xiaohong Jiang,** College of Medicine, Jiaxing University, Jiaxing, China, e-mail: jxh@zjxu.edu.cn
Zhongfei Shen, Bin Shen, Ying Sun: College of Medicine, Jiaxing University, Jiaxing, China

1 Introduction

Sodium aescinate is a sodium salt containing ester bonded triterpenoid saponins. It is a white or quasi-white crystalline powder with a bitter and spicy taste. This compound is derived from the mature, dried seeds of the Chestnut plant. It exhibits a range of pharmacological properties, including the mitigation of inflammation and reduction of fluid exudation. Additionally, it has been found to enhance venous tension, thereby improving blood circulation. Notably, it also plays a role in ameliorating brain function abnormalities [1–3]. Its main active ingredients are sodium aescinate A, B, C, and D [4,5]. However, as the polyester bond in sodium aescin for injection is highly irritating to blood vessels, intravenous injection may cause pain at the injection site, and long-term medication may cause phlebitis. Therefore, strict observation should be made during infusion to prevent the liquid from leaking into surrounding tissues and causing redness and swelling [6]. At the same time, it is required to choose a thicker vein for intravenous infusion and different venipuncture to avoid inconvenient treatment. Second, it is prone to foam in preparation, and sodium aescinate for injection exerts systemic effects after intravenous injection, with poor specificity of the lesion site [7].

Solid lipid nanocarriers (SLNs) have been recognized for their notable aptitude in the encapsulation of a diverse range of drug molecules, both lipophilic and hydrophilic in nature, as detailed in refs [8–11]. This capability extends to the meticulous regulation of drug release and the targeted delivery of these therapeutic agents to specific cells and tissues. The primary composition of SLNs is based on solid lipids, which are stable in a solid state at room temperature. These lipids predominantly consist of long-chain saturated fatty acids, serving as their foundational components, as noted in ref. [12]. The long degradation time of these saturated lipids plays a significant role in ensuring that the release of the drugs within the vesicles is slow and sustained over a long period, thus increasing the therapeutic efficiency over a specified duration. The lipid excipients that are used in the SLNs are a major determinant of

the biological behaviour and the fate of the drug molecules that are loaded into the solid crystalline matrix of the SLNs. This composition is essential in modulating the bioavailability and pharmacodynamics of the drugs as they move across various physiological compartments. In addition to this, the route of administration is another parameter that affects the effectiveness of SLNs as drug delivery carriers, which is important for maximal therapeutic efficacy. The SLN interaction with different components present in biological fluids can cause degradation of these nanoparticles or corona formation on their surface that may significantly modify their physicochemical properties and functionalities. These are important effects and are discussed in refs [13,14].

Lipid-based nanoparticulate formulations have gained increasing attention in the area of pharmaceutical delivery systems, especially for the oral delivery of drugs with low solubility in aqueous media. The relationship between these formulations and the digestive environment is an area of great concern. It is worth mentioning that large lipidic excipients contained in these formulations are known to stimulate the production of bile salts and digestive enzymes in the gastrointestinal tract according to ref. [15]. This process leads to the development of lipid digestion products that are vital in improving the solubilization of drug molecules and their further absorption. Of the many lipid-based delivery systems, SLNs are unique due to their exceptional ability to modulate the release of encapsulated drugs. This fine tuning is very important in regulating the peak concentration of drugs in the blood stream, which is important in minimizing the risk of toxicity that is associated with high drug concentrations. In the pharmacokinetic context, the delay in maximum concentration of drug in plasma time (T_{max}) has been observed in a number of studies, including those cited in ref. [16]. In this study, T_{max} with SLNs was 4.0 h, which was much higher than the 1.7 h noted for the microemulsion formulation. Such observation further highlights the importance of SLNs in sustaining drug release [17]. In addition, pharmacodynamic studies have repeatedly showed that the application of SLNs in oral drug delivery prolongs the therapeutic action of the drugs, providing a desirable sustained release, which is useful in long-term treatment approaches.

In order to solve the irritant problem of drugs, this article proposes a solution to change the drug carrier to improve the targeting of drugs in clinical treatment while maintaining the advantages of the existing preparations such as long and timely curative effect. As drug carriers, SLN can improve the shortcomings of the original therapeutic agents while ensuring the therapeutic effect [18–20]. The irritating problem of sodium aescinate can be alleviated by coating it with solid lipid nanoparticles. The development of preparation expands the development and selection of dosage forms, reduces the pain of medication, enhances the patient's medication compliance, and improves the treatment effect and cure rate.

2 Materials and methods

2.1 Experimental material

Instruments used were BS224S electronic analysis balance (Beijing Setoris Instrument System Co., Ltd), RCT Magnetic Agitator (IKA), Infinity 1260 High Performance Liquid Chromatograph (Agilent Technology Co., Ltd), particle size and surface potential tester (3000HS, Malvem Co., UK), THZ-92A constant temperature oscillator (Haibo Sun Industrial Co., Ltd, Medical equipment factory), Starter 3C pH meter (Shanghai Ohaus Instrument Co., Ltd), Cascada.LS pure water meter (Pall Filter (Beijing) Co., Ltd), separation funnel, and test tube with plug.

Sodium aesculin raw materials (China National Institute of Food and Drug Control, Lot No. 100346-201703; content: 33.5% aesculin A, 31.4% aesculin B, 17.8% aesculin C, and 14.2% aesculin D) and *n*-octanol (Shanghai Maclin Biochemical Technology Co., Ltd) were used.

Forty SPF male BALB/C mice, weighing 20–25 g, were provided by Zhejiang Academy of Medical Sciences with production license No. SCXK (Zhejiang) 2019-0002.

2.2 Study on physicochemical properties of sodium aescinate

Purified water and buffer solutions of pH 4.0, 6.8, and 9.0 were mixed with the same amount of *n*-octanol in conical bottles and placed in a 37°C constant temperature oscillator. Continuous oscillation enabled the solution to maximize saturation with *n*-octanol [4]. Weigh a certain amount of sodium aescinate API, add the same amount of fully saturated solution, and configure the solution with drug concentration of 2.5 mg/mL. Remove 5 mL of each prepared solution into 10 mL corked test tube, and keep the volume constant. The sealing film was sealed and placed in a thermostatic oscillator to oscillate for 2 h before centrifugation. After standing, water phase was absorbed to determine the absorbance, and the concentration was determined by HPLC.

2.3 Determination of sodium aescinate

2.3.1 Chromatographic conditions

Eclipse XDB-C18 (5 μm, 150 × 4.6 mm^2) column; mobile phase: acetonitrile 0.55%, phosphoric acid 37:63; flow rate: 0.8 mL/min; column temperature: 30°C; injection volume: 20 μL; detection wavelength: 220 nm.

2.3.2 Standard curve drawing

Standard sodium aescinate of 25.00 mg was precisely weighed into a 10 mL conical flask, and a certain amount of methanol was added to fully dissolve it, and 2.50 mg/mL of sodium aescinate solution was prepared using a volumetric flask as a reserve solution. The right amount of the reserve liquid is accurately absorbed and diluted with methanol to prepare a series of concentration solutions. According to chromatographic conditions, the standard curve was drawn with peak area as ordinate and sodium aescinate concentration as abscissa.

2.4 Preparation of sodium aescinate solid lipid nanoparticles

2.4.1 Selection of oil phase

By studying the physical and chemical properties and methodology of sodium aescinate, and considering the safety of injection preparation, the oil phases to be selected are soybean oil (injection level) and medium chain triglyceride (injection level), the temporary fixed surfactant is 15-hydroxystearate polyethylene glycol ester and the cosurfactant is glycerol. The ratio of surfactants to cosurfactants is 2:1 (mass ratio). After the surfactant is mixed, it is precisely weighed with the oil phase to be selected, and mixed according to 9:1, 8:2, 7:3, 6:4, 5:5, 4:6, 3:7, 2:8, and 1:9 (mass ratio). Then it is continued to stir and titrated with water for injection. When the system is no longer clear and turbidity occurs, it immediately stops dripping and the amount added is recorded. The mass percentage of oil, water, and mixture at the final critical point was calculated and the data were input to OriginPro 2021 to draw a pseudo-terpolymer phase diagram. The oil phase was determined using the microemulsion area as the selection criteria [5].

2.4.2 Sodium aescinate solid lipid nanoparticles were prepared by high pressure homogenization method

Take a certain amount of emulsifier and oil phase, in 75 ± 5°C water bath and make it completely molten liquid. As the organic phase, take a certain amount of Poloxamer 188 dissolved in 10 mg/mL sodium heptanoside citrate solution; as the water phase, stir at 2,000–4,000 rpm, slowly inject the organic phase into the water phase. Continue stirring for 8–10 min, and quickly cool to room temperature to obtain colostrum. Colostrum was homogenized at 20,000 Pa at room temperature for 3–5 times under high pressure and cooled overnight with ice water bath [6].

2.5 Preparation evaluation of sodium aescinate solid lipid nanoparticles

2.5.1 Determination of particle size and zeta potential

At room temperature, appropriate amount of the newly prepared sodium aescinate solid lipid nanoparticles was taken, and purified water was mixed. The particle size and zeta potential were determined by particle size and surface potentiometer.

2.5.2 Determination of encapsulation rate and drug load

About 1 mL of solid lipid nano-suspension of sodium aescinate was precisely taken and placed in a centrifuge tube, and centrifuged at 10,000 rpm at 4°C for 5 min at high speed. The supernatant was removed, diluted with methanol, and the amount of free drug W_1 was calculated. About 1 mL of solid lipid nanoparticle suspension of sodium aescinate was precisely removed and centrifuged at 3,000 rpm for 15 min. The precipitate was taken and properly diluted with methanol. The sample was determined and the free drug amount W_2 was calculated. In addition, 1 mL of solid lipid nanoparticle suspension of sodium aescinate was precisely removed, and methanol solution was added, which was demulsified and dissolved under ultrasonic conditions, diluted with methanol and fixed volume. Drug concentration was determined according to HPLC methodology, and total drug dosage (W_3), encapsulation rate (EE), and drug loading (DL) were calculated [7]. The calculation formula is EE = $(W_3 - W_1 - W_2)/W_3 \times 100\%$; DL = $(W_3 - W_1 - W_2)/$

$W_4 \times 100\%$, where W_1 and W_2 are free drug amount, W_3 is the total dosage, and W_4 is lipid mass.

2.6 Evaluation of anti-inflammatory activity of sodium aescinate solid lipid nanoparticles

A total of 40 mice were equally distributed into five distinct groups based on their body weights, with each group comprising eight mice. These groups included a blank control, a high-dose, and a low-dose group receiving the commercial sodium aescinate injection, and another set of high-dose and low-dose groups administered with a solid lipid nanosuspension of sodium aescinate. After normal feeding for a period of time, the mice were given intravenous administration according to group arrangement, and the blank control group was given intravenous injection of a certain amount of normal saline. After 30 min of intravenous injection, 0.03 mL of xylene was applied to the right ear of each mouse. After 15 min, the mice were sacrificed, and the two auricular plates were weighed at the same position with a hole punch with a diameter of 0.6 cm, and the difference between auricular plates was regarded as the degree of swelling. The right ear piece was taken from the same position with a hole punch of 0.6 cm in diameter, cut into pieces, and soaked in 5 mL of acetone: water (7:3) sealed for 48 h. The samples were centrifuged at 3000 revolutions per minute (RPM) for 5 minutes, the absorbance of supernatant was measured by 590 nm UV spectrophotometer.

3 Results

3.1 Oil water partition coefficient of sodium aescinate

The determination results of oil–water distribution coefficient of sodium aescinate are shown in Table 1. The oil–water partition coefficient is the ratio of the concentration of *n*-octanol to water phase in the equilibrium of organic compounds, which is determined to simulate the distribution of drugs in water phase and biological phase in the body, so as to predict the absorption of drugs in the body. As can be seen from the table, sodium aescinate is more distributed in the oil phase under acidic conditions.

Table 1: Oil–water distribution coefficient of sodium aescinate in different solutions

	Absorbance	$K_{o/w}$	Log $K_{o/w}$
Purified water	0.711	0.049	−1.309
pH = 4.0	0.087	16.261	1.211
pH = 6.8	0.422	0.734	−0.134
pH = 9.0	0.500	0.201	−0.696

3.2 Determination of sodium aescinate saponin

The chromatography conditions were carefully established, with the medium being an Eclipse XDB-C18 column 5 μm, 150 × 4.6 mm^2. Operational parameters were set at flow rate 0.8 mL/min, column temperature 30 °C. The sample injection volume under the protocol was 20 μL, with the detection wavelength set at 220 nm. Under these chromatographic

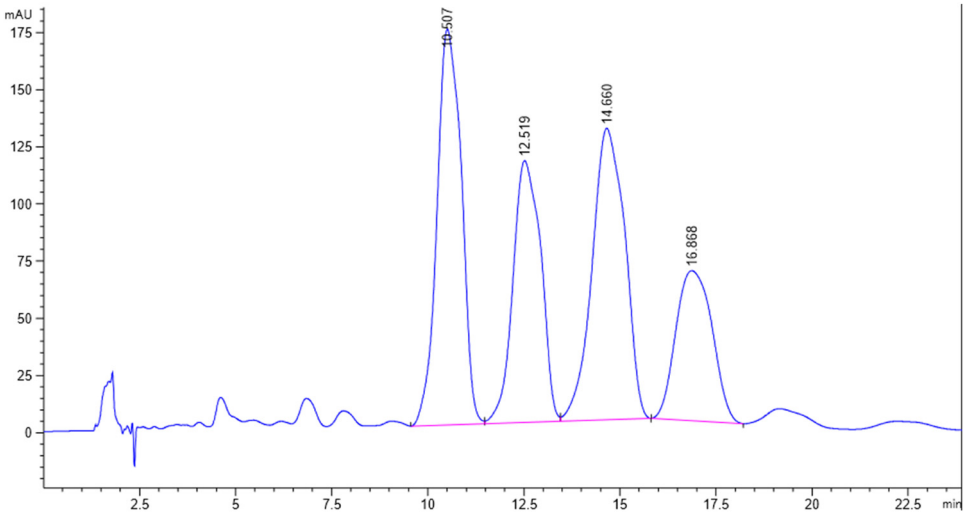

Figure 1: Comparison curve of sodium aescinate.

conditions, the chromatographic peaks of sodium aescinate A, B, C, and D were, respectively (Figure 1). The regression equation of aescinin A was $y = 585.29x - 508.21$ ($R^2 = 0.9911$). When the range of aescinin A was 1.68–16.75 μg, there was a good linear relationship between the peak area and the sample quantity. The regression equation of aescinin B was $y = 481.55x - 412.82$ ($R^2 = 0.9902$). When the range of aescinin B was 1.57–15.70 μg, there was a good linear relationship between the peak area and the sample size. A certain concentration of sodium aescinate reference solution was configured, and six consecutive samples were injected as shown in Table S1.

3.3 Selection of oil phase

As shown in Figure 2, in the microemulsion area, namely the area on the right side of the curve, it can be seen that the same amount of oil solubilizes more surfactant and water mixtures, so mid-chain triglyceride is selected as the oil phase. The optimal formulation ratio is achieved when medium-chain triglycerides are used as a co-solvent in the oil phase. The desired solid lipid nanoparticles of sodium aescinate are obtained through high-pressure homogenization.

3.4 Preparation evaluation of sodium aescinate solid lipid nanoparticles

The sodium aescinate solid lipid nanoparticles underwent a detailed characterization process, focusing on their particle size and zeta potential, with the results being comprehensively depicted in Figure 3. Upon analysis of the graphical representation, it is observed that the nanoparticles possess a notably uniform particle size distribution, with an average dimension calculated to be approximately 142.32 ± 0.17 nm. The zeta potential, an indicator of the stability of these nanoparticles, was measured to be 1.60 ± 0.32 mV. These data suggest a stable colloidal system. Further insights gained through transmission electron microscopy (TEM) provide a vivid illustration of the nanoparticles' spherical morphology. The TEM images distinctly show that these nanoparticles are efficient carriers, encapsulating a substantial amount of drug particles within their structure. Additionally, the research progressed to assess the sodium aescinate solid lipid nanoparticles in terms of their encapsulation efficiency and capacity for drug loading, as outlined in Table 2. Results from this analysis indicated that the nanoparticles exhibited an encapsulation efficiency of 73.93 ± 4.65% alongside a drug loading capacity of 13.41 ± 1.25%. It is noteworthy that these parameters exhibited only minimal variation across different production batches, indicating a high degree of reproducibility in the nanoparticle formulation process.

3.5 Inhibition of ear swelling induced by xylene

The experimental results of inhibiting ear swelling induced by xylene are shown in Table 3. Compared with the blank control group, both aescinin and aescinin solid lipid nanoparticles for injection had inhibiting effect on ear swelling, while the intervention group of aescinin solid lipid nanoparticles had more significant intervention effect ($P < 0.001$), and compared with the low-dose group, the high-dose group had better efficacy.

3.6 Antagonistic effect of drugs on increased capillary permeability induced by xylene

The experimental results of antagonistic effect of drugs on the increase of capillary permeability induced by xylene are shown in Table 4. Compared with the blank control group, both sodium aescine for injection and solid lipid

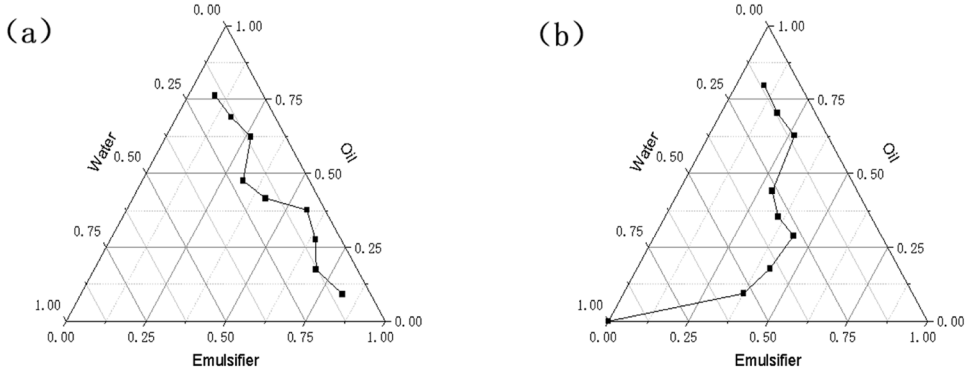

Figure 2: Pseudo-ternary phase diagram of oil phase screening: (a) soybean oil was used as the oil phase and (b) medium-chain triglycerides were used as the oil phase.

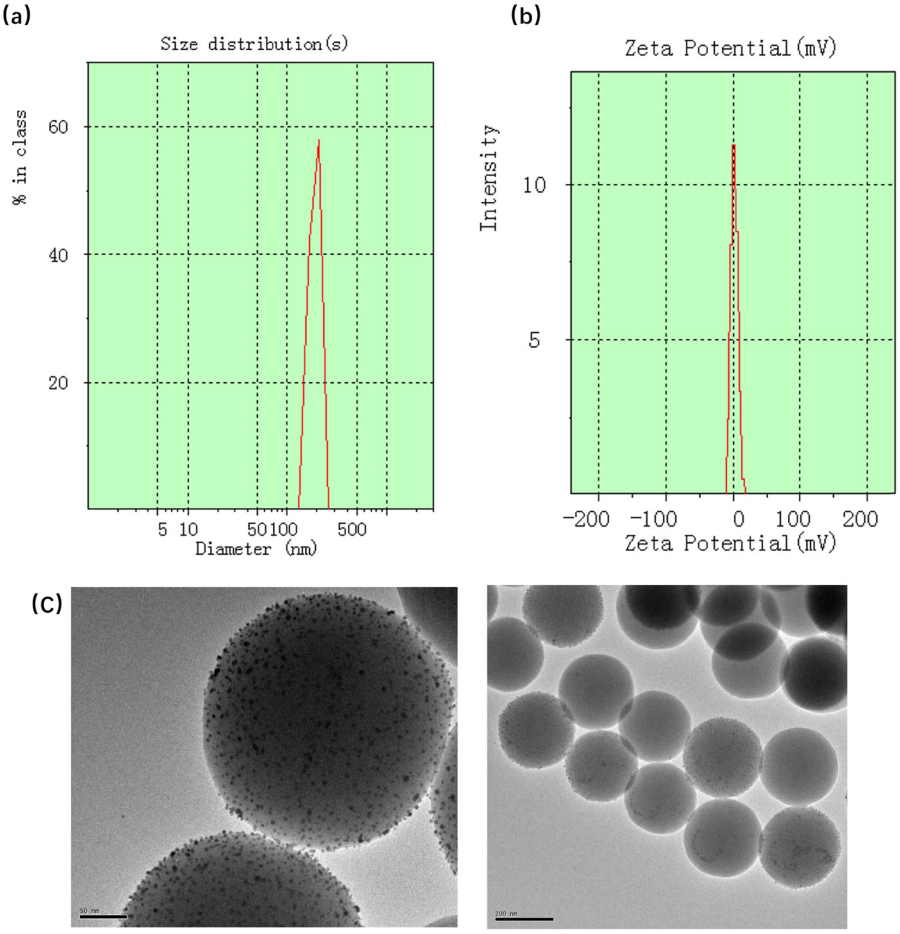

Figure 3: Particle size of sodium aescinate solid lipid nanoparticles (a), surface potential (b), and transmission electron microscopy (c).

Table 2: Determination results of encapsulation rate and drug load

Batch	Encapsulation rate (%)	Drug load (%)
1	73.4 ± 3.80	12.68 ± 0.94
2	74.1 ± 4.48	15.59 ± 1.32
3	74.3 ± 5.67	11.95 ± 1.48

nanoparticles of sodium aescine for injection have antagonistic effect on the increase of capillary permeability. However, compared with the sodium aescine for injection group, the sodium aescinate solid lipid nanoparticles intervention group did not show a more significant intervention effect, and compared with the low-dose group, the high-dose group did not show a significant effect.

4 Discussion

SA, a sodium salt derivative of a triterpenoid saponin, is obtained from the desiccated mature fruits of the Chinese Buckeye Seed. Documented in refs [21,22], this compound is

Table 3: Experimental results of ear swelling induced by xylene

The name of the drugs	Dosage (mg/kg)	Swelling degree (mg)	*P* values
Sodium aescinate for injection	1.0	14.62 ± 2.37	<0.05
	5.0	12.43 ± 1.66	<0.01
Sodium aescinate solid lipid nanoparticles	1.0	12.81 ± 3.12	<0.01
	5.0	10.55 ± 2.24	<0.001
Blank control group		20.11 ± 1.87	

Table 4: Experimental results of ear permeability induced by xylene

The name of the drugs	Dosage (mg/kg)	Absorbance	*P* values
Sodium aescinate for injection	1.0	0.125 ± 0.044	<0.05
	5.0	0.106 ± 0.029	<0.01
Sodium aescinate solid lipid nanoparticles	1.0	0.114 ± 0.051	<0.05
	5.0	0.093 ± 0.037	<0.05
Blank control group		0.191 ± 0.072	

recognized for its pharmacological prowess, notably its anti-inflammatory, anti-osmotic, and anti-swelling capabilities. In the sphere of clinical medicine, SA has gained prominence for its effective management of edema and hematoma across various anatomical regions. Its utility extends to addressing a spectrum of conditions, encompassing acute and chronic tissue damage, bone fractures, and trauma. Furthermore, SA is effective in treating brain dysfunctions arising from a multitude of causative factors and ameliorating local blood circulation issues linked to a variety of vascular diseases, as elucidated in ref. [23]. Empirical evidence from clinical trials underscores the stability, efficacy, and reliability of SA as an anti-inflammatory and anti-swelling agent. SA's versatility is evident in its various pharmaceutical forms, including liniments, gels, tablets, and injections, each finding a widespread application in clinical settings. Notably, its topical formulations, such as liniments and gels, have demonstrated commendable therapeutic outcomes in the treatment of superficial injuries like ecchymoses, sprains, and crush injuries. However, it is important to recognize that these external applications, despite their effectiveness, come with certain limitations.

The partition coefficient between oil and water, denoted as K_o/w, quantifies the equilibrium distribution of organic molecules across *n*-octanol and water phases. This coefficient is assessed to model the dispersion of pharmaceuticals between aqueous environments and biological matrices in a living organism, thereby facilitating predictions regarding the bioavailability of these substances [24,25]. The drug must be water-soluble and fat-soluble in order to be absorbed through the biofilm [26]. In this study, we found that the distribution of sodium aescinate in the oil phase is more under acidic condition.

SA tablets are convenient for oral administration, but their limited absorption and low bioavailability restrict their efficacy [27]. Conversely, SA-I is characterized by its swift initiation of action coupled with an extended period of sustaining biological effects. This attribute renders it efficacious in managing and mitigating post-surgical swelling as well as in alleviating pain among patients [28,29]. Meanwhile, the intravenous application of SA-I was accompanied by discomfort at the injection site, which is the result of the pronounced irritant effect of septate sodium on the circulatory system. Increased use of this agent may increase the risk of phlebitis. Taking into account the above-mentioned limitations, a thorough analytical study was launched in order to improve the assay for sodium ginsenoside. See the Methods section for specific conditions. The system's suitability tests were performed to determine its ruggedness, which provided for the high reproducibility of injections and the stability of analytical solutions under these conditions.

By the study of formulation of sodium aescinate solid lipid nanoparticles, we determined the oil phase for the chain triglyceride, emulsifier for soybean phospholipids and 15-hydroxy stearic acid polyglycol ester (1:2), we found that the optimal ratio of prescription for high pressure homogeneous sample of legal system, the high pressure homogeneous method to get the further perfect, the necessary sodium aesculin solid lipid nanoparticles were prepared. Our results also showed that sodium aescin solid lipid nanoparticles injection had a smooth appearance, presenting a uniform and stable milky white suspension with an average particle size of 142.32 ± 0.17 nm and zeta potential of 1.60 ± 0.32 mV. Transmission electron microscopy showed that the particle size was uniform, the distribution of encapsulated drugs was uniform, and the encapsulation rate and drug loading of sample preparation were good [24,30–32]. According to Tables 3 and 4, both high and low doses of sodium aescinate for injection and solid lipid nanoparticles of sodium aescinate had a good inhibitory effect on ear swelling induced by xylene in mice, and had a good antagonistic effect on the increase of capillary permeability induced by xylene. Analysis shows that the inhibition and antagonism of sodium aescinate solid lipid nanoparticles are more obvious. Therefore, preliminary pharmacodynamics results showed that compared with sodium aescinate for injection, solid lipid nanoparticles of sodium aescinate had a better anti-inflammatory activity [33].

5 Conclusion

The results of this research reveal that a relatively refined method for determining sodium aescinate content has been established, and a reasonable formulation has been selected for the preparation of sodium aescinate solid lipid nanoparticles. The average particle size was 142.32 ± 0.17 nm, the zeta potential was 1.60 ± 0.32 mV, and the encapsulation rate was 73.93 ± 4.65%. The drug loading was 13.41 ± 1.25%. In conclusion, this method can produce stable solid lipid nanoparticles containing sodium aescinate with uniform particle size, even distribution after encapsulation, and significant anti-inflammatory activity.

Funding information: This investigation was financially supported by Science Technology Department of Zhejiang Province under the project of "Construction of a rat model of osteoarthritis and its application in the evaluation of the

efficacy of aescin sodium solid lipid nanoparticles," with grant number LGD19C040003.

Author contributions: X.H.J. – experimental design and analysis of experimental data; Z.F.S. – manuscript writing, review, and editing; B.S. – experimental work; Y.S. – supervision of experiments and translation.

Conflict of interest: The authors declare no conflicts of interest.

Ethical approval: The animal research was provided by Zhejiang Academy of Medical Sciences with production license No. SCXK (Zhejiang) 2019-0002.

Data availability statement: The datasets generated during and/or analysed during the current study are available from the corresponding author on reasonable request.

References

[1] Li L, Xu B, Li CR, Zhang MM, Wu SJ, Dang WJ, et al. Anti-proliferation and apoptosis-inducing effects of sodium aescinate on retinoblastoma Y79 cells. Int J Ophthalmol. 2020;13(10):1546–53. doi: 10.18240/ijo.2020.10.06.

[2] Huang XJ, Wang DG, Ye LC, Li J, Akhtar M, Saleem S, et al. Sodium aescinate and its bioactive components induce degranulation via oxidative stress in RBL-2H3 mast cells. Toxicol Res. 2020;9(4):413–24. doi: 10.1093/toxres/tfaa042.

[3] Li J, Zheng L, Wang R, Sun D, Liang S, Wu J, et al. Synergistic combination of sodium aescinate-stabilized, polymer-free, twin-like nanoparticles to reverse paclitaxel resistance. Int J Nanomed. 2020;15:5839–53. doi: 10.2147/IJN.S259432.

[4] Liu W, Qin F, Wu F, Feng H, Yang Q, Hou L, et al. Sodium aescinate significantly suppress postoperative peritoneal adhesion by inhibiting the RhoA/ROCK signaling pathway. Phytomedicine. 2020;69:153193. doi: 10.1016/j.phymed.2020.153193.

[5] Zhang L, Fei M, Wang H, Zhu Y. Sodium aescinate provides neuroprotection in experimental traumatic brain injury via the Nrf2-ARE pathway. Brain Res Bull. 2020;157:26–36. doi: 10.1016/j.brainresbull.2020.01.019.

[6] Sun N, Li D, Chen X, Wu P, Lu YJ, Hou N, et al. New applications of oleanolic acid and its derivatives as cardioprotective agents: a review of their therapeutic perspectives. Curr Pharm Des. 2019;25(35):3740–50. doi: 10.2174/1381612825666191105112802.

[7] Sharma N, Zahoor I, Sachdeva M, Subramaniyan V, Fuloria S, Fuloria NK, et al. Deciphering the role of nanoparticles for management of bacterial meningitis: an update on recent studies. Environ Sci Pollut Res Int. 2021;28(43):60459–76. doi: 10.1007/s11356-021-16570-y.

[8] Tapeinos C, Battaglini M, Ciofani G. Advances in the design of solid lipid nanoparticles and nanostructured lipid carriers for targeting brain diseases. J Control Release. 2017;264:306–32. doi: 10.1016/j.jconrel.2017.08.033.

[9] Muller RH, Mader K, Gohla S. Solid lipid nanoparticles (SLN) for controlled drug delivery – a review of the state of the art. Eur J Pharm Biopharm. 2000;50(1):161–77. doi: 10.1016/s0939-6411(00)00087-4.

[10] Mu H, Holm R. Solid lipid nanocarriers in drug delivery: characterization and design. Expert Opin Drug Deliv. 2018;15(8):771–85. doi: 10.1080/17425247.2018.1504018.

[11] Christophersen PC, Zhang L, Mullertz A, Nielsen HM, Yang M, Mu H. Solid lipid particles for oral delivery of peptide and protein drugs II – the digestion of trilaurin protects desmopressin from proteolytic degradation. Pharm Res. 2014;31(9):2420–8. doi: 10.1007/s11095-014-1337-z.

[12] Gamboa CK, Samir R, Wu C, Mu H. Solid lipid particles as drug carriers – effects of particle preparation methods and lipid excipients on particle characteristics. Pharm Nanotechnol. 2018;6(2):124–32. doi: 10.2174/2211738506666180420165547.

[13] Ke PC, Lin S, Parak WJ, Davis TP, Caruso F. A decade of the protein corona. ACS Nano. 2017;11(12):11773–6. doi: 10.1021/acsnano.7b08008.

[14] Maretti E, Rustichelli C, Lassinantti Gualtieri M, Costantino L, Siligardi C, Miselli P, et al. The impact of lipid corona on rifampicin intramacrophagic transport using inhaled solid lipid nanoparticles surface-decorated with a mannosylated surfactant. Pharmaceutics. 2019;11(10):508. doi: 10.3390/pharmaceutics11100508.

[15] Mu H, Holm R, Mullertz A. Lipid-based formulations for oral administration of poorly water-soluble drugs. Int J Pharm. 2013;453(1):215–24. doi: 10.1016/j.ijpharm.2013.03.054.

[16] Gaur PK, Mishra S, Bajpai M, Mishra A. Enhanced oral bioavailability of efavirenz by solid lipid nanoparticles: in vitro drug release and pharmacokinetics studies. Biomed Res Int. 2014;2014:363404. doi: 10.1155/2014/363404.

[17] Zhang Q, Yie G, Li Y, Yang Q, Nagai T. Studies on the cyclosporin a loaded stearic acid nanoparticles. Int J Pharm. 2000;200(2):153–9. doi: 10.1016/s0378-5173(00)00361-6.

[18] Sommonte F, Arduino I, Racaniello GF, Lopalco A, Lopedota AA, Denora N. The complexity of the blood–brain barrier and the concept of age-related brain targeting: challenges and potential of novel solid lipid-based formulations. J Pharm Sci. 2022;111(3):577–92. doi: 10.1016/j.xphs.2021.08.029.

[19] Parvez S, Yadagiri G, Arora K, Javaid A, Kushwaha AK, Singh OP, et al. Coalition of biological agent (melatonin) with chemotherapeutic agent (amphotericin B) for combating visceral leishmaniasis via oral administration of modified solid lipid nanoparticles. ACS Biomater Sci Eng. 2023;9(6):2902–10. doi: 10.1021/acsbiomaterials.1c00859.

[20] Wibel R, Braun DE, Hammerle L, Jorgensen AM, Knoll P, Salvenmoser W, et al. In vitro investigation of thiolated chitosan derivatives as mucoadhesive coating materials for solid lipid nanoparticles. Biomacromolecules. 2021;22(9):3980–91. doi: 10.1021/acs.biomac.1c00776.

[21] Costantini A. Escin in pharmaceutical oral dosage forms: quantitative densitometric HPTLC determination. Farmaco 1999;54(11–12):728–32. doi: 10.1016/s0014-827x(99)00090-7.

[22] Song XH, Wang WH, Chen ST, Chen S, Zhang J, Wang YS, et al. Application of high performance liquid-ion trap mass spectrometry in analyzing saponins in sodium aescinate. Zhongguo Zhong Yao Za Zhi. 2016;41(13):2449–54. doi: 10.4268/cjcmm20161313.

[23] Arnould T, Janssens D, Michiels C, Remacle J. Effect of aescine on hypoxia-induced activation of human endothelial cells. Eur J Pharmacol. 1996;315(2):227–33. doi: 10.1016/s0014-2999(96)00645-0.
[24] Cizmar P, Yuana Y. Detection and characterization of extracellular vesicles by transmission and cryo-transmission electron microscopy. Methods Mol Biol. 2017;1660:221-32. doi: 10.1007/978-1-4939-7253-1_18.
[25] Guo Y, Ma S, Guan S, Zhang Y, Pan J. High-throughput determination of octanol-water partition coefficients by ultrasound-assisted liquid-phase microextraction. J Chromatogr Sci. 2015;53(8):1400–6. doi: 10.1093/chromsci/bmu218.
[26] Rakshasbhuvankar A, Patole S, Simmer K, Pillow JJ. Enteral vitamin A for reducing severity of bronchopulmonary dysplasia in extremely preterm infants: a randomised controlled trial. BMC Pediatr. 2017;17(1):204. doi: 10.1186/s12887-017-0958-x.
[27] Wu XJ, Zhang ML, Cui XY, Gao F, He Q, Li XJ, et al. Comparative pharmacokinetics and bioavailability of escin Ia and isoescin Ia after administration of escin and of pure escin Ia and isoescin Ia in rat. J Ethnopharmacol. 2012;139(1):201–6. doi: 10.1016/j.jep.2011.11.003.
[28] Wang B, Yang R, Ju Q, Liu S, Zhang Y, Ma Y. Clinical effects of joint application of beta-sodium aescinate and mannitol in treating early swelling after upper limb trauma surgery. Exp Ther Med. 2016;12(5):3320–2. doi: 10.3892/etm.2016.3743.
[29] Banwell HA, Paris ME, Mackintosh S, Williams CM. Paediatric flexible flat foot: how are we measuring it and are we getting it right? A systematic review. J Foot Ankle Res. 2018;11:21. doi: 10.1186/s13047-018-0264-3.
[30] Harris JR. Transmission electron microscopy in molecular structural biology: a historical survey. Arch Biochem Biophys. 2015;581:3–18. doi: 10.1016/j.abb.2014.11.011.
[31] Mohammadian S, Agronskaia AV, Blab GA, van Donselaar EG, de Heus C, Liv N, et al. Integrated super resolution fluorescence microscopy and transmission electron microscopy. Ultramicroscopy. 2020;215:113007. doi: 10.1016/j.ultramic.2020.113007.
[32] Hunziker P, Schulz A. Transmission electron microscopy of the phloem with minimal artifacts. Methods Mol Biol. 2019;2014:17–27. doi: 10.1007/978-1-4939-9562-2_2.
[33] Sarris J. Herbal medicines in the treatment of psychiatric disorders: 10-year updated review. Phytother Res. 2018;32(7):1147–62. doi: 10.1002/ptr.6055.